Taylor & Francis
Taylor & Francis Group

International Journal of Pavement Engineering

ISSN: (Print) (Online) Journal homepage: https://www.tandfonline.com/loi/gpav20

Optimisation of recycled concrete aggregates for cement-treated bases by response surface method

Kondeti Chiranjeevi, Doma Hemanth Kumar, Anil Sagar Srinivasa & A. U. Ravi Shankar

To cite this article: Kondeti Chiranjeevi, Doma Hemanth Kumar, Anil Sagar Srinivasa & A. U. Ravi Shankar (2023) Optimisation of recycled concrete aggregates for cement-treated bases by response surface method, International Journal of Pavement Engineering, 24:1, 2179051, DOI: 10.1080/10298436.2023.2179051

To link to this article: https://doi.org/10.1080/10298436.2023.2179051

Published online: 17 Feb 2023.

INTERNATIONAL JOURNAL OF PAVEMENT ENGINEERING
2023, VOL. 24, NO. 1, 2179051
https://doi.org/10.1080/10298436.2023.2179051

Taylor & Francis
Taylor & Francis Group

Check for updates

Optimisation of recycled concrete aggregates for cement-treated bases by response surface method

Kondeti Chiranjeevi, Doma Hemanth Kumar, Anil Sagar Srinivasa and A. U. Ravi Shankar

Department of Civil Engineering, National Institute of Technology Karnataka, Mangaluru, India

ABSTRACT
Sustainability is a primary concern that needs to be addressed since infrastructure development requires significant natural resources. Using Recycled Concrete Aggregates (RCA) for road construction has numerous benefits in saving natural resources and the environment. In the present investigation, the demolition waste is being used for road construction, partially/fully replacing natural aggregates. The Cement Treated Recycled Concrete Aggregate (CTRCA) specimens were prepared at 3%, 5%, and 7% cement with various blends of RCA and Natural Coarse Aggregates (NCA) ranging from 0 to 100%. The strength characteristics in terms of Unconfined Compressive Strength (UCS), Flexural Strength (FS), Elastic Modulus, Indirect Tensile Strength (ITS) and durability tests were conducted on cured samples. Microstructural analysis using Scanning Electronic Microscope (SEM) revealed that the pores and cracks in the old mortar have a detrimental influence on the mechanical properties of CTRCA mixes. However, Energy Dispersive Spectroscopy (EDS) and durability tests have shown positive results. The Response Surface Method (RSM) was utilised to optimise the RCA and cement content in CTRCA mixes. The research resulted in the maximum possible RCA of up to 70% with a cement content of 5.8%, which met the Indian Road Congress (IRC) specifications for Cement Treated Bases (CTB).

ARTICLE HISTORY
Received 26 October 2022
Accepted 6 February 2023

KEYWORDS
Ball-milling; recycled concrete aggregate; cement treated bases; response surface method; sustainability

Introduction

The demolition waste generated from old structures is inevitable due to economic development and technological advancement. More than half of global demolition waste comes from China, India, and the United States of America, with concrete waste accounting for up to 67% of total demolition waste (Chung and Lo 2003, Akhtar and Sarmah 2018). Every year, more than 6 billion tonnes of concrete is produced worldwide (Ä *et al.* 2012). This waste is disposed of in dumping yards, water bodies, drain trenches, and untilled grounds around human habitations.

Furthermore, accumulating demolition waste in landfills tends to inhabit vacant land that could have been used for other purposes. These waste materials have become vital resources increasingly in road construction due to the scarcity of natural resources. Recycling aggregates from construction and demolition waste is the sole solution to conserve traditional aggregates and safeguard the environment. The potential application of RCA in base and sub-base pavement courses will solve disposal problems and conserve natural resources (Leite *et al.* 2011, Arulrajah *et al.* 2014). It is necessary to characterise RCA before its use in pavements. A crucial factor influencing the performance of pavements is the particle size distribution. Different crushing techniques and the concrete's strength are responsible for the variances in the particle size distribution of RCA (Aydilek.pdf n.d., Arulrajah *et al.* 2012, Gabr and Cameron 2012). The density of RCA is lower than NCA because of the attached mortar content on its surface (Tang *et al.* 2018).

Clay bricks and RCA were utilised for unbound flexible pavement as an alternative material. It was found that crushed clay brick experienced an increase in Optimum Moisture Content (OMC) and a subsequent decrease in Maximum Dry Density (MDD) (Poon and Chan 2006). The RCA absorbs more water than conventional materials; a greater OMC is needed to achieve MDD for RCA than NCA (Cardoso *et al.* 2016). However, California Bearing Ratio (CBR) was less than NCA but within permissible limits (Aghililotf *et al.* 2021). An increase in modified proctor density resulted in increased CBR value, and the soaking effect on CBR is negligible. The Resilient Modulus (M_R) measures the elastic behaviour of paving materials under repeated wheel loads (Gabr and Cameron 2012, Rahman *et al.* 2014).

The Repeated Load Triaxial Test (RLTT) test is frequently used to forecast aggregate stiffness and permanent deformation behaviour under a range of applied stress. Blending 25% RCA with 75% NCA would produce the same elastic behaviour and permanent deformation as a Dense Graded Aggregate Base. The shape of the RCA and the strength of the parent concrete affect the M_R values (Nataatmadja and Tan 2001). Several studies revealed that RCA exhibited higher M_R and permanent deformation than NCA (Aydilek.pdf n.d., Bestgen *et al.* 2016). The UCS and M_R of cement-stabilised RCA show a V-shaped variation, with increased RCA content for the curing period of fewer than 60 days and decreasing after 90 days (Hou *et al.* 2019). Few researchers conclude that plastic strain was not influenced by moisture content above OMC (Jayakody *et al.* 2019).

CONTACT Kondeti Chiranjeevi chiru854@gmail.com

The highway engineers developed stabilising soils and aggregates for use in pavements over the years. The CTB mixture is a cementitious material consisting of aggregate, Cement, and water that stiffens after compaction. The CTB mixtures differ entirely from concrete in their particle size distribution, Cement content, water content, and specimen preparation.

Further Cement treated materials have superior flexural fatigue and load-bearing capacity than unbound materials (Jofre and Kraemer 2008). Moreover, the cement stabilisation increases the base rigidity and decreases the deflections. Cement stabilisation improves the service life of pavements under higher traffic loads (Eren and Filiz 2009). Compaction characteristics play a significant role in achieving the excellent compactability of the bases. Due to the attached mortar content, the RCA mixes have higher OMC and lower MDD than NCA. Finding the OMC for the combinations of RCA may be quite challenging due to the variations in the attached mortar content on the surface of RCA.

Earlier investigations on recycled aggregates for sub-base and base layers reported that mixed recycled aggregate has low optimal density compared to natural aggregates because of the attached mortar content on the surface of the aggregate (Agrela *et al.* 2012). Based on the investigation of Ebrahim Abu El-Maaty Behiry (2013) and Lim and Zollinger (2003), the UCS is the primary measure to assess the strength of the cement-treated mixtures. The UCS improved with increased RCA content up to 75% replacement of conventional aggregates and lowered at 100% RCA when stabilised with 5% cement. A few researchers found that 75% of NCA can be replaced with RCA if the parent concrete strength is high (Toka and Olgun 2021). The cement-treated mixes exhibited improved UCS at a 5% fines content than at a 10% fines level. Tensile strength, which is the potential to resist bending, is an essential attribute of the cement-treated bases because it allows the pavement to bend in response to traffic movements. The ITS and flexural stiffness of cement-treated mixtures increased when the specimen was tested with the increase in cement content and decreased with RCA content (Ebrahim Abu El-Maaty Behiry 2013). The Modulus of resilience for RCA is greater than that of NCA, and RCA is susceptible to moisture. Blending RCA and NCA may not reduce permanent deformation (Haider *et al.* 2014). The toughness modulus and compressive strength of cement-stabilised RCA were increased by adding more than 1.5% polyvinyl alcohol (Yaowarat *et al.* 2022).

Few researchers studied laboratory fatigue characteristics using the four-point bending flexural test and an indirect tensile test. Then laboratory fatigue life was compared with the Accelerated Loading facility test (Yeo 2008). The fatigue resistance of Cement treated bases under the same applied strain level, the beam specimens with high cement content exhibited more fatigue life (Dong *et al.* 2021). The fatigue performance of Cement stabilised aggregates reinforced with polypropylene filament fibre was improved by 1.0–4.2 times compared with conventional Cement stabilised aggregates (Peng and Qingfu 2009). The hydration reaction of the Cement, the amount of fine aggregate, the amount of water in the mix, and the density of the mix all significantly impact the crack resistance of CTB (George 1990). Numerous studies have found that adding fibres to the Cement stabilised macadam can improve resistance to cracking and shrinkage properties (Maduabuchukwu Nwakaire *et al.* 2020).

Even though a substantial study has been done on RCA utilisation in CTB, no specific optimum RCA replacement and cement content are recommended for using RCA in CTB. However, designing CTB with RCA as a replacement for NCA is complicated due to the significant heterogeneity of the material properties used in their production and the limited knowledge of the interactions among mix design variables. The incorporation of RCA for the bound pavement lower layers has been observed in various studies (Mohammadinia *et al.* 2015, 2016, Arulrajah *et al.* 2016, Mohammadinia *et al.* 2019a, 2019b). Li *et al.* (2021) used RSM to optimise and assess the impacts of several elements, i.e. independent variables, on a given process, either individually or in combination. The RSM is an optimisation method that integrates statistical and mathematical tools for experiment design, model fitting, regression analysis, and independent variable interaction analysis (Li *et al.* 2021). When multiple factors and levels are involved, RSM can solve the problem of a persistent response by setting up a functional relationship between contextual variables and response values. It fits the regression equation to draw the response surface and contour line for each factor level. In parallel, the optimum prediction value is determined based on the response of each factor level, providing optimisation design benefits over the single factor control variable approach and orthogonal test. The Central Composite Design (CCD) and Box–Behnken Design (BBD) are two standard designs of RSM widely used in multi-objective optimisation in the area of material engineering (Shi *et al.* 2022). Mohammed *et al.* (2017) developed the prediction models of cast in-situ alkali-activated binders with a Face-centered Central Composite Design (FCCD) for two factors with three levels each (Mohammed *et al.* 2019).

Significance of the present study

For designing a flexible pavement with Cement treated material as base or sub-base, it is necessary to evaluate the FS and durability of the material along with UCS. The mechanical properties of CTRCA are essential for assessing the optimum mixes of RCA and NCA. However, limited research has been carried out considering all the properties of the mix proportioning. In order to evaluate the efficiency of Cement stabilised layers along with RCA and NCA, it is necessary to consider the properties like OMC, MDD, ITS, FS, Modulus of Elasticity and UCS. The present study adopts the FCCD in RSM to optimise the RCA and Cement content. The microstructural characteristics of CTRCA mixes were examined. The optimal mix proportions are validated from the experimental results and can be adopted for the sub-base/base layers.

Materials

The materials utilised to make CTRCA specimens are NCA, RCA, Cement, and water. Demolition waste was collected from a nearby area and crushed into small pieces. Jaw crushing was employed to crush small pieces into the required sizes

Table 1. Physical properties of RCA and NCA.

Property	NCA	RCA	Specification as per MoRTH (2013)
Water Absorption, %	0.6	2.7	2
Aggregate Impact Value (AIV), %	23.0	29	40
Specific Gravity (G)	2.65	2.42	NA
Los Angeles Abrasion Value, %	28	31	35
Combined Flakiness and Elongation Index, %	27	29	35

further. The aggregates obtained from jaw crushers have more mortar content attached to the surface. The adhered mortar on the aggregate surface was removed partly by subjecting it to the ball milling process. The appropriate charge, revolution time and weight of aggregates for the ball milling process are fixed based on the number of trials. The achieved weight of aggregates of 6, 3 kg charge and revolution time of 20 min resulted in less water absorption. The physical properties of both NCA and RCA were evaluated and tabulated in Table 1. The aggregates were blended to achieve the desired gradation suggested by MoRTH (2013), and the results are depicted in Figure 1. All the blends are within limits recommended by MoRTH (2013). Ordinary Portland Cement 43 grade was used in the current study. Potable water was used to prepare CTRCA specimens in the present study.

Methodology

Establishment of statistical models employing the RSM

In the present study, RSM is used to develop a relationship between variables and outcomes and examine the effect of RCA and cement contents on the performance of CTRCA mixtures. The RSM is an essential statistical technique connecting each response to many variables to identify the interactions, relationships, and effects between the variables and responses. It has the benefit of examining the influence of numerous variables on the responses and optimising the response value (Kockal and Ozturan 2011, Martinez-Conesa *et al.* 2017). The design, numerical modelling, statistical analysis, and optimisation of the process factors were done using the Design-Expert software. In the present investigation, mix design formulations of CTRCA mixtures are chosen randomly based on the FCCD for two independent variables. The RCA content ranges from 0 to 100%, and cement content ranges from 3% to 7% by dry weight of aggregate is considered, and the variation has been presented in Table 2. The interaction and relationship between the process variables, RCA proportion, cement content, and the response may be ascertained using Analysis of Variance (ANOVA) (Rezaifar *et al.* 2016).

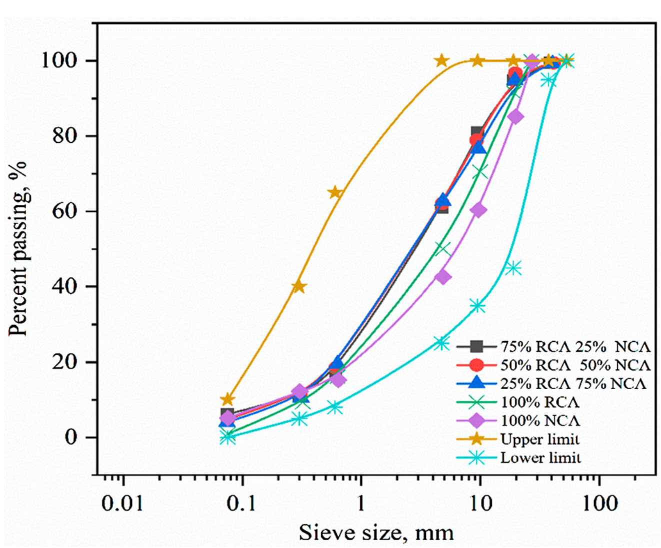

Figure 1. Grain size distribution curves for RCA and NCA blends.

Specimen preparation

For Cement treated recycled aggregate mixes, the OMC and MDD were determined per ASTM D1557-07 (2014). The RCA and NCA were thoroughly mixed based on moisture content and cement content varying from 3 to 7% to attain the desired blend. Cylindrical specimens of a diameter of 100 mm and height of 200 mm and a beam of a breadth of 100 mm, a height of 100 mm and a length of 500 mm were cast using a table vibratory compactor. After 24 h, the specimens were de-moulded and cured for seven and 28 days. The specimens were cured with covering gunny bags and sprinkled with water at regular intervals till the completion of the curing period.

Evaluation of CTRCA mixtures

Unconfined compressive strength. For any stabilised material, the pavement design depends on the UCS values of the material used (Congress 2018). Accordingly, the test was carried out on 7 days and on 28 days of cured cylindrical CTRCA samples as per ASTM C39-01 (2003). A compressive load machine of 2000 kN capacity with a rate of loading 0.5 kN/s was used to test the UCS samples.

Flexural strength. The performance of the bound layer depends primarily on FS. The standard test method as per ASTM C-78 was adopted to test the FS of the CTRCA mixtures (ASTM C-78 2018). The third point loading test was conducted on the beam specimens. The FS value was computed using Equation (1).

$$\mathrm{FS} = \frac{PL}{bd^2} \tag{1}$$

where L is the length between rollers (mm); d is the depth (mm); b is the width (mm); P is the failure load (N).

Elastic modulus. Elastic Modulus of CTRCA mixtures was conducted on beam specimens per IRC SP 89 (IRC SP 89_Part 1 2010). A hydraulic loading system was used to apply load at a constant rate of 1.25 mm/min. Deflections were measured by dial gauges fixed at the Centre of the beam. Load versus deflection graphs were plotted. The Elastic Modulus of the CTRCA specimens was determined after the test using Equation (2).

$$E = \frac{\mathrm{Pa(L2 - 4a2)}}{24 * I} \tag{2}$$

where P = Failure load (N); L = Effective length (mm); I = Moment of inertia (mm^4); a = L/3 (mm).

Table 2. Mix formulation of CTRCA mixtures.

	Source material		
Mix ID	RCA %	NCA %	Cement %
RCA0NCA100C3	0	100	3
RCA0NCA100C5	0	100	5
RCA0NCA100C7	0	100	7
RCA25NCA75C3	25	75	3
RCA25NCA75C5	25	75	5
RCA25NCA75C7	25	75	7
RCA50NCA50C3	50	50	3
RCA50NCA50C5	50	50	5
RCA50NCA50C7	50	50	7
RCA75NCA25C3	75	25	3
RCA75NCA25C5	75	25	5
RCA75NCA25C7	75	25	7
RCA100NCA0C3	100	0	3
RCA100NCA0C3	100	0	5
RCA100NCA0C3	100	0	7

Indirect tensile strength. The ITS values of CTRCA mixtures were evaluated as per ASTM C-496 and IS 5816: 1999 (IS 5816, 1999, ASTM C496 2020). A hydraulic loading test set up with a capacity of 6000 kN was used to test the 7-day cured cylindrical specimens. The ITS values are evaluated using Equation (3)

$$ITS = \frac{2P}{\pi DL} \tag{3}$$

where L = Specimen length (mm); D = Specimen diameter (mm); P = Ultimate load (N); ITS in N/mm^2 or MPa.

Durability studies. A durability test was carried out to assess cement-treated materials' ability to withstand severe environmental conditions. A simple wetting and drying test was conducted on CTRCA mixes as per Indian Standard (IS): 4332 (Part IV) (IS 4332 Part 4 1968). In each cycle, the sample was immersed in water for five hours to replicate the wetting condition and kept in the oven at 70°C for about 42 h. The percentage weight loss was measured, and the same procedure continued until the sample failure, or 12 cycles that occurred, was first noticed as the durability of the CTRCA specimen.

Results and discussions

Effect of RCA content and cement content on OMC and MDD

The OMC and MDD for the blends of RCA and NCA with varying cement content were evaluated, and the results are depicted in Figure 2(a,b), respectively. The MDD and OMC values of all the mixtures are in the range of 20.32–23.65 kN/m^3 and 5.9–9.8%, respectively. Further, the mix RCA100NCA0C3 showed the minimum MDD value of 20.32 kN/m^3 at its OMC of 8.8%. It is evident that with an increase in RCA, the MDD decreases. Further, a 2-dimensional plot was used to illustrate the established model contour plot, as seen in Figure 2(c,d).

The fact that the contour lines were all elliptical suggests that the RCA and cement content significantly affect the mixes. It has been observed that the model depicts the perfect interaction between the independent variables. In Figure 2(c), the yellowish area denotes a good blend that results in the desired OMC values. The green region in Figure 2(d) indicates the desired MDD values of the CTRCA mixes.

Effect of RCA and Cement on UCS. The UCS tests were conducted on the CTRCA mixtures at various percentages of

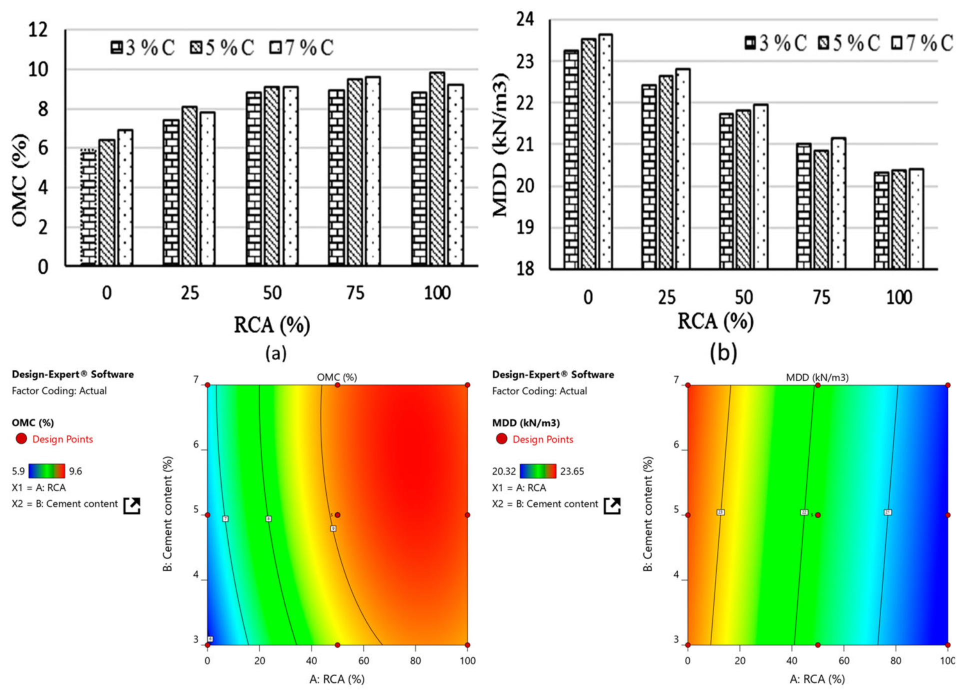

Figure 2. (a) Optimum moisture content and (b) Maximum dry density of CTRCA mixes. (c) Contour plot for optimum moisture content of CTRCA mixes. (d) Contour plot for maximum dry density of CTRCA mixes.

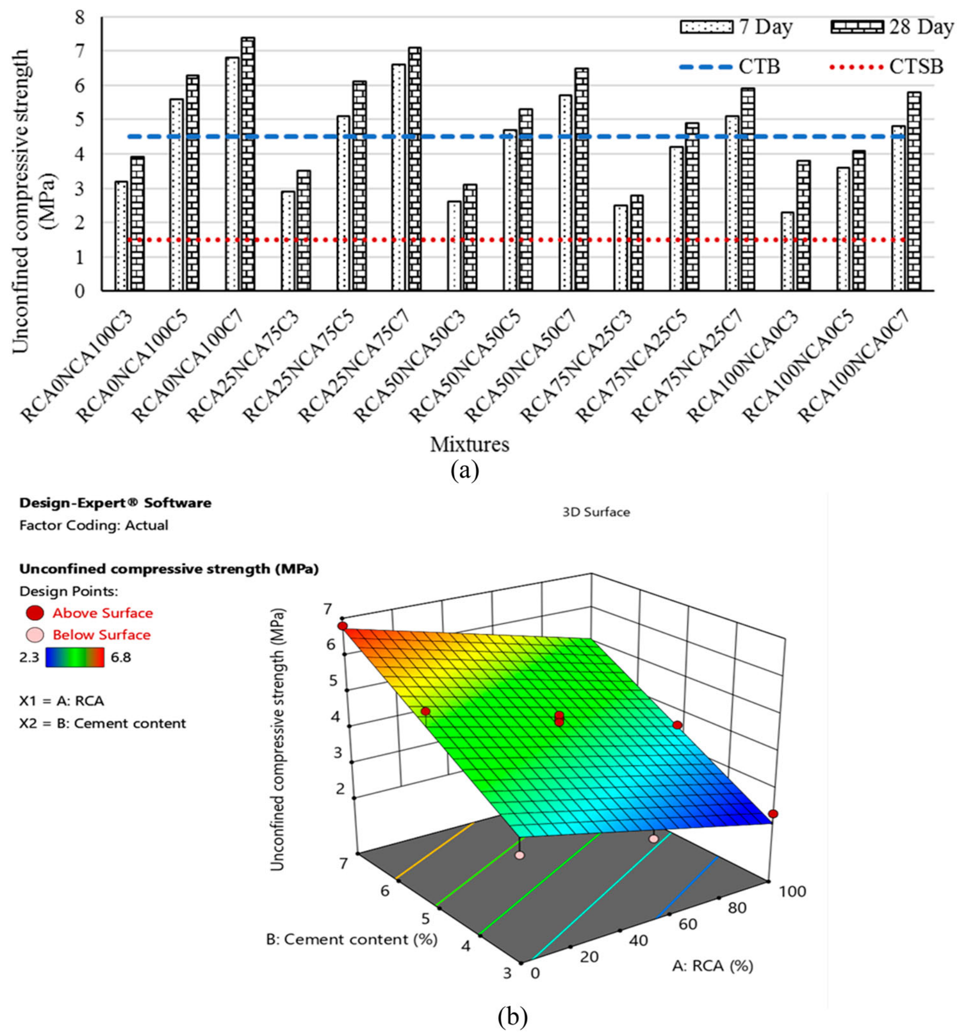

Figure 3. (a) Unconfined compressive strength of CTRCA mixes. (b) 3D plot for unconfined compressive strength of CTRCA mixes.

RCA and cement contents, and the results are depicted in Figure 3(a). The UCS values vary from 2.3–6.8 MPa after seven days of curing.

The mix RCA0NCA100C7 exhibited a maximum UCS value of 6.8 MPa. The minimum UCS of 2.3 MPa was observed for the mix RCA100NCA0C3. There is an improvement in UCS values with increased cement content and a decrease in RCA content, and the same observation is made by (Ebrahim Abu El-Maaty Behiry 2013). The mix exhibited lower UCS due to the attached mortar content on the RCA surface, leading to a weak Interfacial Transition Zone (ITZ). This old ITZ is the weakest part of the matrix, which fails early compared to the new ITZ. In the mix with 100 per cent RCA for the cement content of 3%, 5%, and 7%, the obtained UCS values are reduced by 28%, 35% and 29%, respectively. The increase of UCS with the curing period was significant for 5% and 7% cement content compared to the conventional mix. In Figure 3(b), the greenish part indicates the appropriate variable combination, which gives optimum strength values. The reddish portion indicates higher UCS values with increased cement content, and the bluish region shows lower UCS values with increased RCA%. Figure 3(b) represents the influence of the synergy between RCA replacement and Cement on the UCS. When Cement is constant, with an increase in RCA, the UCS decreases by 30–40%. The weak ITZ between the aggregate and matrix, higher concrete porosity, reduced strength of RCA, and the development of microcracks that may weaken the attachment around aggregate are some potential causes of this strength reduction. Similarly, with the increased cement content, the compressive strength increased by 40–50% when RCA was unchanged. IRC 37-2018 recommended 7 d UCS value of 1.5 MPa to 3.0 MPa for Cement treated subbase material and 4.5–7.5 MPa for CTB layers (MoRTH 2013, Congress 2018).

Effect of RCA content and cement content on indirect tensile strength

The ITS tests were conducted on CTRCA; the results are depicted in Figure 4(a). The ITS values for the seven days cured CTRCA samples are in the range of 0.25–0.8 MPa. The mix RCA0NCA100C3 has a minimum ITS value of 0.25 MPa, while RCA0NCA100C7 has a maximum ITS value of 0.8 MPa.

There is a significant decrease in ITS value at lower cement content and higher RCA%, which is evident in Figure 4(a). As RCA increases, the ITS values decrease, and with the increase

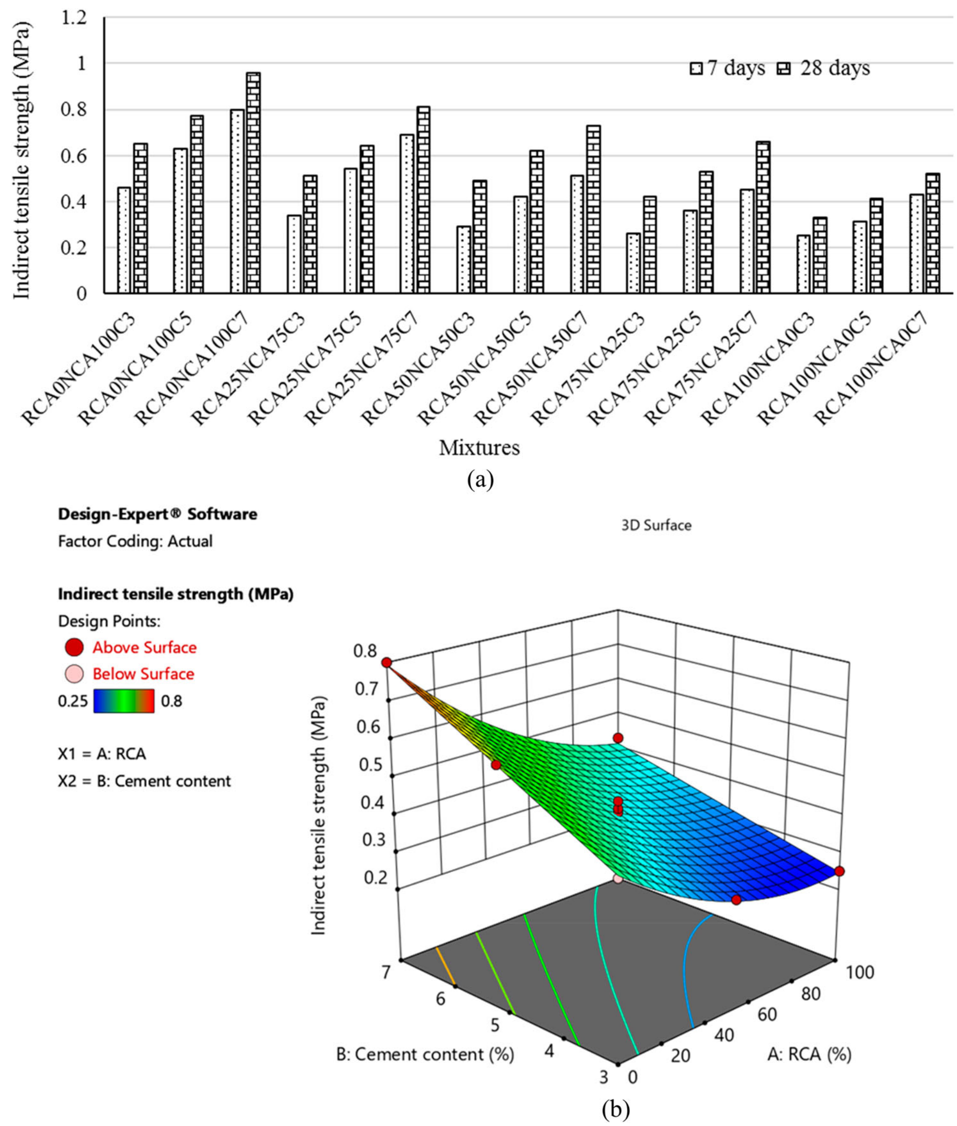

Figure 4. (a) Indirect tensile strength of CTRCA mixes. (b) 3D plot for indirect tensile strength of CTRCA mixes.

in cement content, the ITS improves. The dispersion of pores in the RCA structure and increasing porosity may cause a decrease in strength. The influence of the two parameters (RCA and Cement) on the ITS after seven days of curing is depicted in a three-dimensional (3D) graphic in Figure 4(b). The bluish-green section of Figure 4(b) denoted the appropriate variable combination.

The reddish part indicates higher ITS values with increased cement content, and the bluish part shows lower ITS values with increased RCA%. At constant Cement content, with an increase in RCA up to 100%, ITS reduces by 45–50%. The mortar adhered to aggregates is a weak point and lowers the ITS. It must develop a smoother zone near ITZ in to increase performance. ITS increases by 20–35% with an increase in Cement when RCA replacement remains unchanged.

Effect of RCA and cement percentage on flexural strength

The FS tests were conducted on RCA mixes. The FS of CTRCA samples cured for seven days varies from 0.48 to 1.98 MPa and is evident from Figure 5(a). At a fixed RCA content, the FS of CTRCA mixes improved with an increase in cement content, which is evident from Figure 5(c). The mix RCA0NCA100C7 exhibited a maximum FS of 1.98 MPa. At constant cement content, as RCA increases, the FS values decrease. The minimum value of 0.48 MPa was observed for the mix RCA100NCA0C3. In the mix with 100% RCA for the cement content of 3%,5%, and 7%, the obtained FS values are reduced by 25%, 21%, and 33%, respectively, compared to the conventional mix. The possible reason for low FS may be cracks and pores on the surface of RCA, resulting in weak bonding with the new matrix. The failure of the old ITZ occurring before the new ITZ results in reduced FS. The effect of the RCA replacement and cement content on the seven days FS is depicted in Figure 5(b). The greenish-yellow area in Figure 5(b) represented the desired variable combination, suggesting that RCA and Cement interact very well. The reddish part indicates higher FS values with increased cement content, and the bluish part shows lower FS values with increased RCA%. The mixes with an FS of more than 1.45 MPa can be recommended for the base layer (Congress 2018).

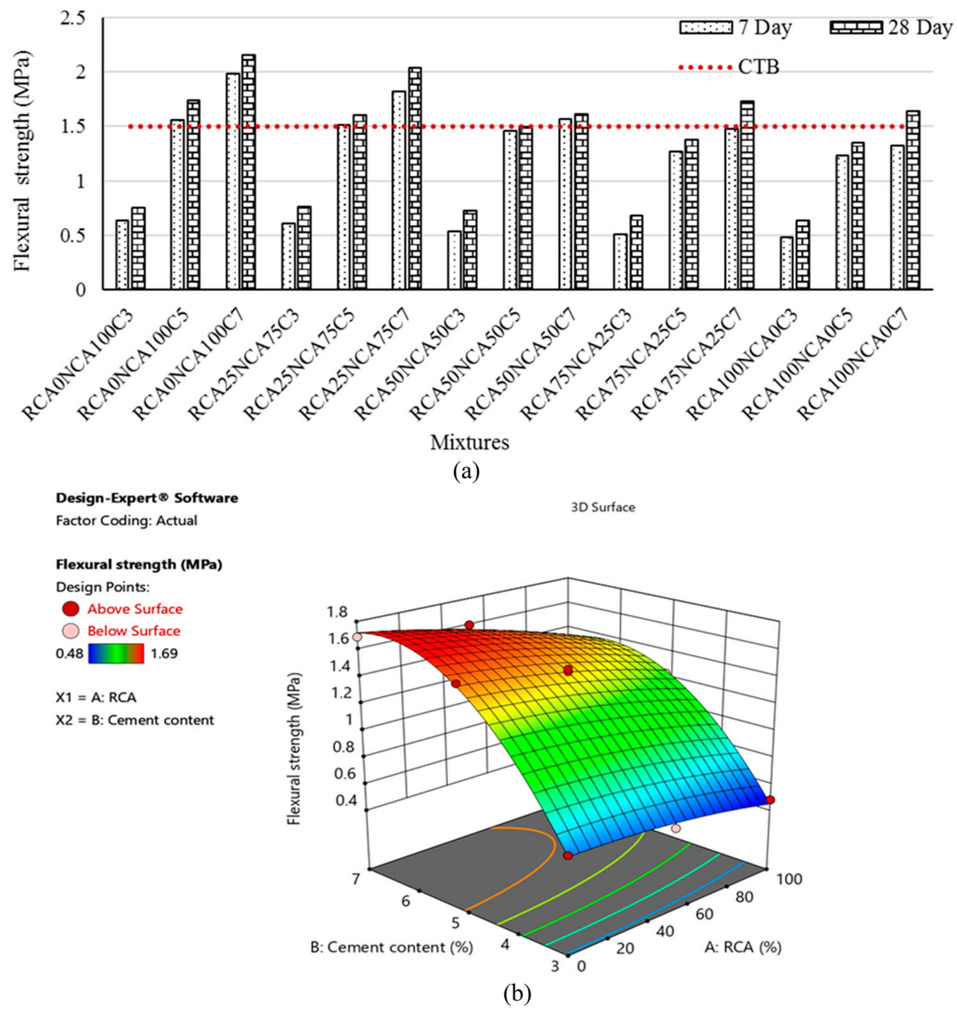

Figure 5. (a) Flexural strength of CTRCA mixes. (b) 3D plot of flexural strength of CTRCA mixes.

Effect of RCA and cement on elastic modulus

The Elastic Modulus values of the CTRCA mixtures at different replacements of RCA and various cement contents are shown in Figure 6(a). The Elastic Modulus of CTRCA mixes ranges from 852 to 2182 MPa after 28 days of curing. The Elastic Modulus of CTRCA mixes increases with an increase in cement content at a constant RCA, which is depicted in Figure 6(a). The mix RCA0NCA100C7 exhibited a maximum value of 2182 MPa. The Elastic Modulus value decreases with an increase in the RCA replacement level. The Elastic Modulus of CTRCA mixes is affected by various factors, including the aggregate density and the transition zone's properties. The porosity and density of the aggregate are key parameters of the bulk matrix stiffness. The mix RCA100NCA0C3 exhibited a low value of 852 MPa.

The greenish-yellow portion of the contour plot in Figure 6(b) indicates a perfect coalescence that yields desired strength values. The reddish part shows the higher modulus values with an increase in cement content, and the bluish portion indicates the lower modulus values with an increase in the RCA replacement level. When cement content is kept constant, with 100% RCA, the Modulus of Elasticity value reduces by 20–25% compared to conventional mix. When RCA remains constant, an increase in cement content improves a 30–50% increase in Elastic Modulus. The coefficient of variation (CV) for all the experimental test results is less than 10%, making the data reliable. Further, the data is optimised using RSM to utilise the maximum possible RCA content in CTB.

Durability test

The durability tests on CTRCA specimens were conducted as per ASTM D-559 (1996). The procedure is repeated for 12 cycles to replicate field conditions. The results show that the mix RCA100NCA0 at 3% cement content was less durable than other mixes. The weight loss for the mixes with 5% and 7% cement contents is marginal, irrespective of RCA replacement. The weight loss for all the mixtures is shown in Figure 7.

The mixtures with weight loss of less than 14% at the end of 12 cycles are considered durable for pavement construction as per IRC guidelines (Congress 2018). In the present study, all the mixtures satisfy the durability criteria.

Microstructural analysis

Scanning electron microscope (SEM) and energy dispersive spectroscopy (EDS). SEM and EDS analysis were conducted

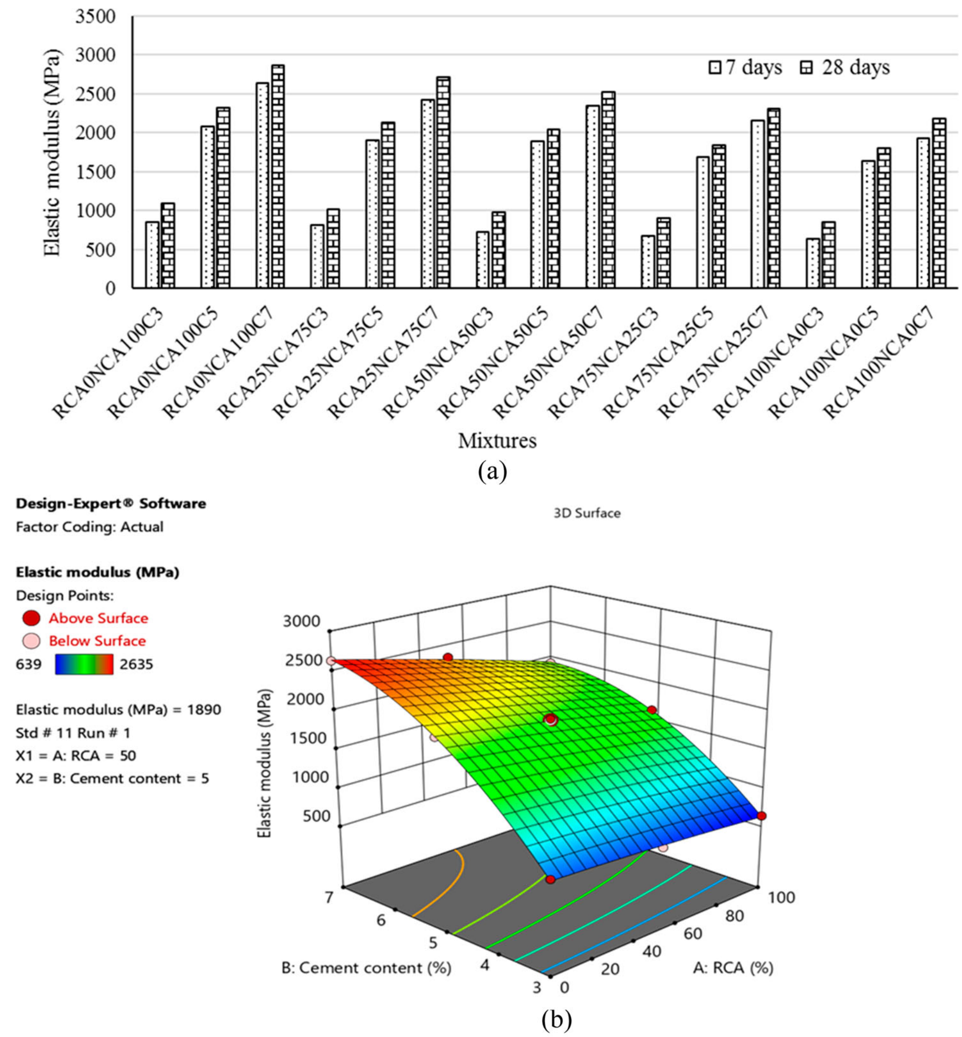

Figure 6. (a) Elastic modulus of CTRCA mixes. (b) 3D plot for elastic modulus of CTRCA mixes.

on the mix with 100% RCA to understand the material's behaviour better. Pores and hydration-related products were detected using SEM images. The bond between the aggregate and cement mortar plays a significant role in determining its mechanical performance. The weak spot of cement-treated mixtures is the ITZ between the cement paste and aggregate. The CTRCA mixtures have two ITZs: an old ITZ between RCA and old adhered mortar, and a new ITZ between RCA and new matrix, as shown in Figure 8, results in lower strength. The constituent elements and their composition in CTRCA mixes were analysed through EDS analysis. Various elements like Si, Ca, and Al of 9.10, 38.56 and 1.69%, respectively,

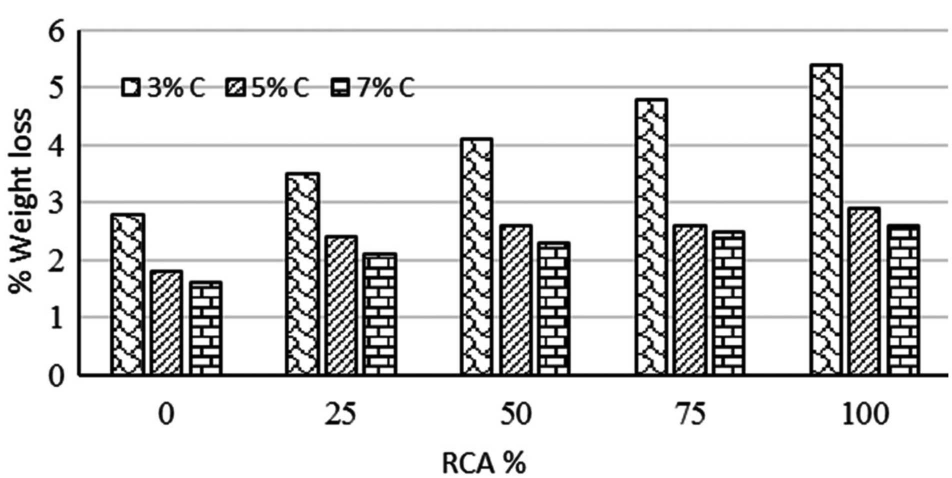

Figure 7. Percentage weight loss in wetting and drying test.

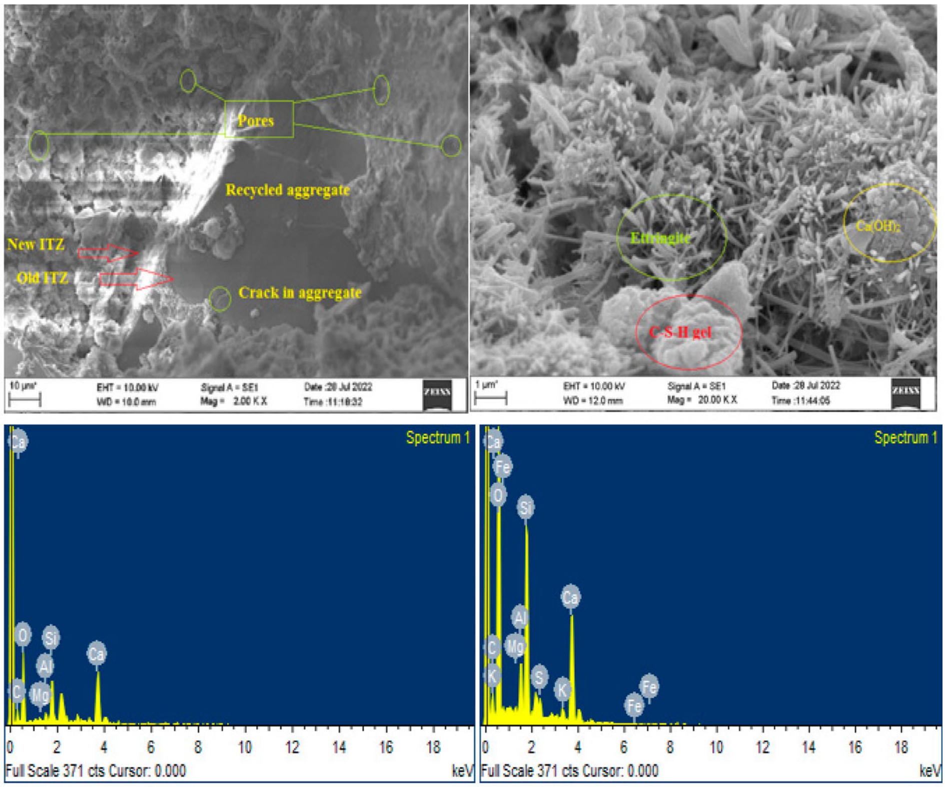

Figure 8. SEM images and EDS analysis of CTRCA mixtures.

were identified in the CTRCA mixtures, which help form hydration compounds (C–S-H, C-A-H and CH). The Si/Ca ratio of the CTRCA mixture was found to be 0.23, which signifies strength and durability. The strength will generally decrease as the Si/Ca ratio increases; in other words, the more calcium present, the more hydration products will occur.

X-ray diffraction analysis (XRD). X-ray diffraction measurements were performed on a Malvern Panalytical Empyrean XRD machine using monochromatic Cu-Kα X-ray diffraction patterns in the range of 2θ from 20° to 70° and a mean scan step of 0.026° and a scan rate of 20°/min. The crystalline phase transitions were examined using the software X'Pert High Score Plus (Panalytical). The addition of Cement enhanced calcium-based compounds resulted in higher-intensity peaks. Figure 9 depicts the formation of C_3S and C_2S, which will help in the strength gain of CTRCA mixes.

Statistical analysis of the experimental data

The developed models are mathematically evaluated and verified. The analysis was conducted at a 5% significance level to examine the significance of experimental factors. UCS, ITS, Elastic Modulus, FS and compaction characteristics are the dependent variables in this study, while RCA content and cement content are the independent variables. The *p*-values reported in Table 3 indicate that each component is

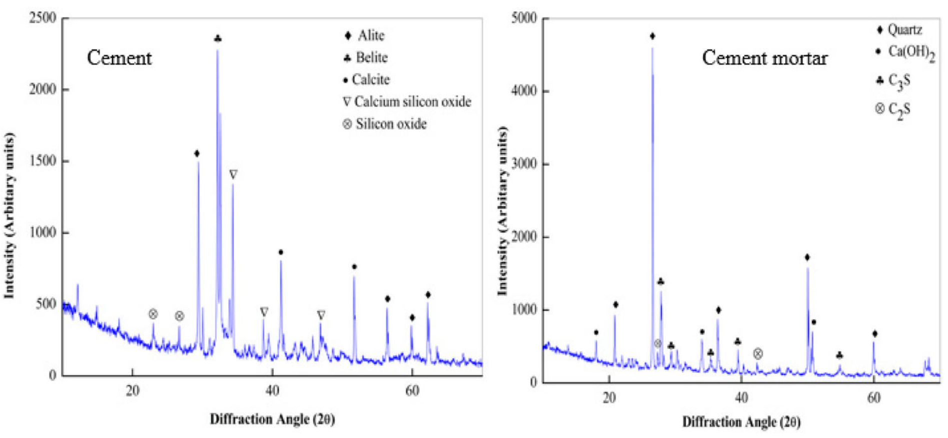

Figure 9. XRD profile for cement and cement mortar.

Table 3. Analysis of response models from ANOVA.

Responses	Source	S. S	Df	M.S	*F*-value	*P*-value	Remark
FS (MPa)	Model	0.2492	5	0.0498	123.86	< 0.0001	significant
	A-RCA	0.1350	1	0.1350	335.57	< 0.0001	
	B-Cement content	0.0913	1	0.0913	226.86	< 0.0001	
	AB	0.0064	1	0.0064	15.91	0.0053	
	A^2	0.0139	1	0.0139	34.64	0.0006	
	B^2	2.956E-06	1	2.956E-06	0.0073	0.9341	
	Residual	0.0028	7	0.0004			
	Lack of Fit	0.0013	3	0.0004	1.20	0.4156	not significant
Elastic Modulus (MPa)	Model	4.445E + 06	5	8.891E + 05	1404.18	< 0.0001	significant
	A-RCA	3.069E + 05	1	3.069E + 05	484.72	< 0.0001	
	B-Cement content	3.679E + 06	1	3.679E + 06	5809.75	< 0.0001	
	AB	60516.00	1	60516.00	95.58	< 0.0001	
	A^2	955.86	1	955.86	1.51	0.2589	
	B^2	3.270E + 05	1	3.270E + 05	516.50	< 0.0001	
	Residual	4432.16	7	633.17			
	Lack of Fit	2662.96	3	887.65	2.01	0.2554	not significant
UCS (MPa)	Model	18.11	2	9.05	105.93	< 0.0001	significant
	A-RCA	4.00	1	4.00	46.82	< 0.0001	
	B-Cement content	14.11	1	14.11	165.04	< 0.0001	
	Residual	0.8547	10	0.0855			
	Lack of Fit	0.6827	6	0.1138	2.65	0.1827	not significant
ITS (MPa)	Model	0.2492	5	0.0498	123.86	< 0.0001	Significant
	A-RCA	0.1350	1	0.1350	335.57	< 0.0001	
	B-Cement content	0.0913	1	0.0913	226.86	< 0.0001	
	AB	0.0064	1	0.0064	15.91	0.0053	
	A^2	0.0139	1	0.0139	34.64	0.0006	
	B^2	2.956E-06	1	2.956E-06	0.0073	0.9341	
	Residual	0.0028	7	0.0004			
	Lack of Fit	0.0013	3	0.0004	1.20	0.4156	not significant

Note: Df: Degree of freedom; P: Probability; F: Fisher statistical value; S.S: Sum of squares; M.S: Mean square.

significant at a 95% confidence level and regarded as a critical factor affecting the experimental results. The R^2 value was used to assess the model quality. The ANOVA data shows the R^2 values for UCS, ITS, FS and Elastic modulus models of 0.9549, 0.9888, 0.9964 and 0.9990, respectively, are tabulated in Table 4. These values indicate a substantial degree of consistency between the expected and test results, and essential to note that the adjusted R^2 and predicted R^2 values coincide well. Also, the difference is less than 0.2, indicating a perfect correlation. The lack of fit could also be used to evaluate model performance; a lower lack of fit value implies a more worthy model (Usman Kankia *et al.* 2021). It was noted that the corresponding *P*-values for the lack of fit test are higher than 0.05, as depicted in Table 3, which shows outstanding fitness for all model responses. Normal probability plots evaluated the distribution of data and validation of sufficiency. The distribution for all dependent variables shows that all residual responses data were distributed normally, as shown in Figure 10. Plots of predicted and actual results assessed the feasibility and capacity of the response models graphically. The anticipated outcomes against the actual results plot show that the predicted response model is accurate. The points are fitted along a straight line, demonstrating a good fit with the experimental data and results predicted by the current models. Variance analysis was used to establish interactions and effects between the variables (A = RCA % and B = cement content %) and responses, as shown in Equations (4)–(8).

All the models except MDD and UCS were quadratic. The linear models for UCS and MDD indicate no significant combined effect of RCA and Cement on the UCS and MDD.

$$\mathrm{OMC}(y_1) = +4.190 + 0.0815\ \mathrm{A} + 0.7209\ \mathrm{B} - 0.0015\ \mathrm{AB} - 0.00046\ \mathrm{A}^2 - 0.0504\ \mathrm{B}^2 \quad (4)$$

$$\mathrm{MDD}(y_2) = +23.0926 - 0.0311\ \mathrm{A} + 0.0600\ \mathrm{B} \quad (5)$$

$$\mathrm{UCS}(y_3) = -1.3602 - 0.01633\ \mathrm{A} + 0.7666\ \mathrm{B} \quad (6)$$

$$\mathrm{ITS}(y_4) = +0.2274 - 0.00384\ \mathrm{A} + 0.07908\ \mathrm{B} + 0.0004\ \mathrm{AB} + 0.000028\ \mathrm{A}^2 + 0.000259\ \mathrm{B}^2 \quad (7)$$

$$\mathrm{FS}(y_5) = -2.1124 + 0.00151\ \mathrm{A}^2 + 1.1888\ \mathrm{B} - 0.00055\ \mathrm{AB} - 0.000017\ \mathrm{A}^2 - 0.091638\ \mathrm{B}^2 \quad (8)$$

$$\text{Elastic modulus}(y_6) = -2.331.91 + 2.3708\ \mathrm{A} + 1313.25\ \mathrm{B} - 0.0074\ \mathrm{A}^2 - 86.0258\ \mathrm{B}^2 \quad (9)$$

Table 4. Characteristics of the model.

Response	UCS (MPa)	ITS (MPa)	FS (MPa)	Elastic Modulus (MPa)
Std. Dev.	0.2924	0.0201	0.0327	25.16
Mean	4.38	0.4415	1.25	1708.77
C.V. %	6.68	4.54	2.62	1.47
R^2	0.9549	0.9888	0.9964	0.9990
Adjusted R^2	0.9459	0.9808	0.9938	0.9983
Predicted R^2	0.9050	0.9442	0.9693	0.9933
Adequate Precision	33.4650	40.1185	57.1634	118.0675

Note: C.V.: Coefficient of variation.

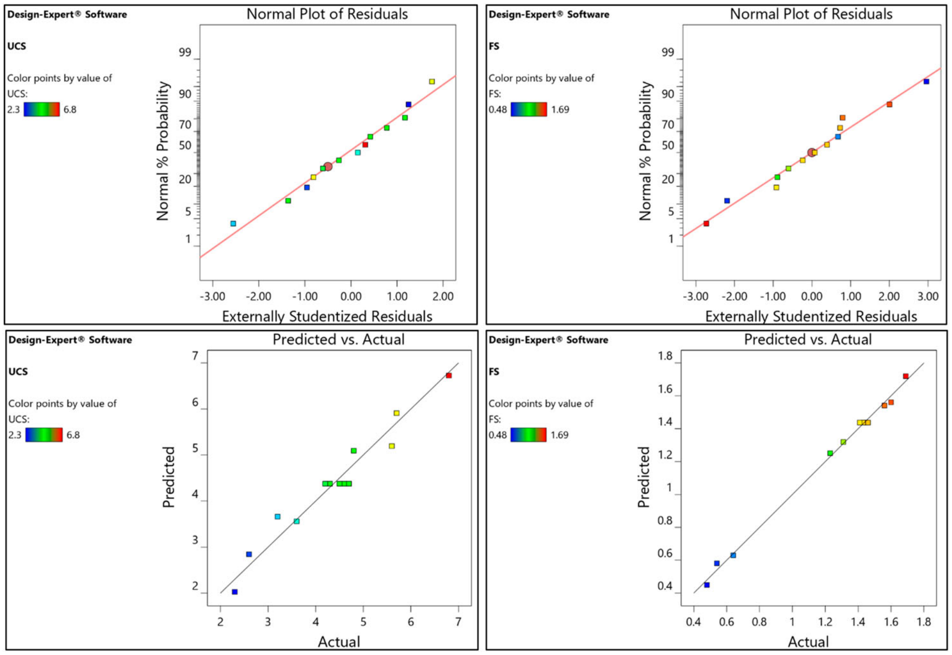

Figure 10. Normal plot of residuals and predicted outcomes vs actual outcomes plots.

Table 5. Optimisation benchmark.

Input Parameters	Goals	Lower limit	Upper limit
A: RCA (%)	Maximise	0	100
B: Cement (%)	Minimise	3	7
y_1: UCS (MPa)	Maximise	4.5	7
y_2: ITS (MPa)	Maximise	0.23	0.8
y_3: FS (MPa)	Maximise	1.45	1.98
y_4: Elastic Modulus (MPa)	Maximise	852	2182

Table 6. Model testing for error.

Responses	RCA (%)	Cement (%)	Experimental results	Predicted results	Error (%)
Compressive strength (MPa)	71	5.8	5.1	4.6	8.4
ITS (MPa)	71	5.8	0.37	0.4	4.0
FS (MPa)	71	5.8	1.58	1.5	5.0
Elastic Modulus (MPa)	71	5.8	1930	2023	4.3

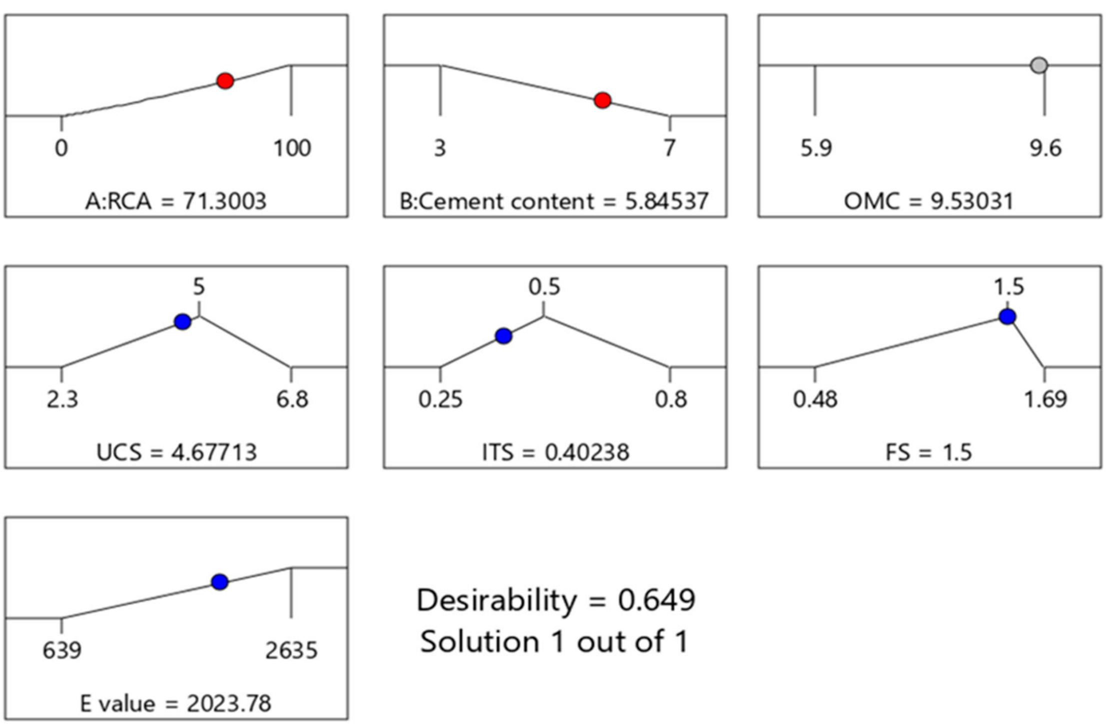

Figure 11. Optimisation ramps.

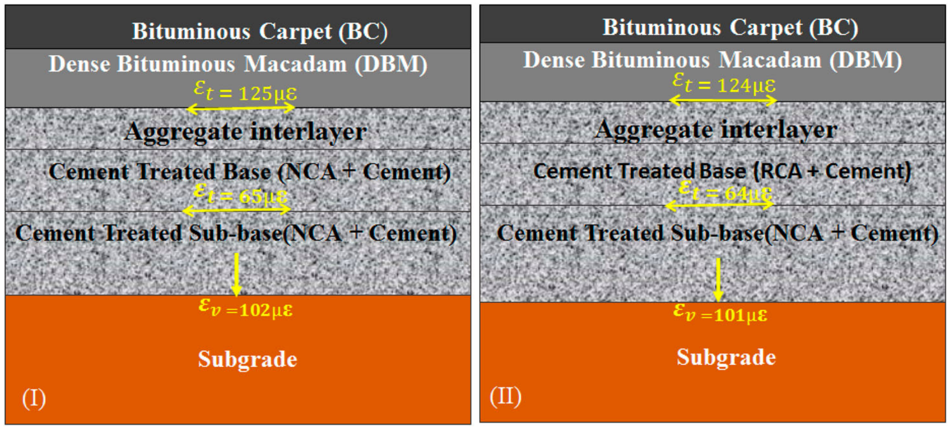

Figure 12. (I) Cement-treated layers with NCA (II) Cement-treated layers with RCA.

Optimisation and validation study. The optimum proportion of RCA and cement content was determined using numerical multi-objective optimisation to maximise the utilisation of RCA% and strength values and minimise the cement content of the CTRCA mixes. The primary goal of the optimisation study is to identify the desirable values of independent variables to achieve the optimisation objectives. Table 5 summarises the optimisation criteria. The RSM technique was used to improve the response affected by various variables. It defined the meaning function for the desired outcome (Mermerdaş *et al.* 2017).

$$\text{Error}(\%) = \frac{\text{Actual value}-\text{predictive value}}{\text{Actual value}} \times 100\% \qquad (10)$$

The optimum proportion of RCA 71% with 5.8% cement content was obtained through numerical optimisation for a desirability functional value of 0.649, showing that the projected value is very reliable (Aydin 2013). The desirability function of a single solution varies between 0 and 1, where 0 represents an unsatisfactory response value, and 1 represents the desired response value. An additional evaluation was accomplished by employing the optimised mixture proportions to validate the adequacy of the optimisation outcomes and all response models. The responses of numerical optimisation solutions are shown in Table 6 based on the optimisation goal. Using Equation (10), the % error between actual and predicted results was assessed and reported, as seen in Table 6. The % error for optimising CTRCA mix proportions is less than 10%, concerning the actual value for optimising the CTRCA mix proportions, which reveals model accuracy high. The optimisation ramps depicted in Figure 11 provided a pictorial representation of the independent factors and responses.

Pavement design and analysis

Pavement analysis and design were carried out for the two base materials, namely (i) Cement treated NCA and (ii) CTRCA, to show the impact of CTRCA mixes on pavement composition. Section I was a conventional flexible pavement composed of Bituminous Carpet (BC), Dense Bituminous Macadam (DBM), aggregate interlayer, Cement treated aggregate base (Cement + NCA), untreated sub-base, and subgrade layers. Flexible pavement consisting of BC, DBM, aggregate interlayer, Cement treated recycled aggregate base (Cement + RCA), untreated sub-base, and subgrade layers were considered section II as depicted in Figure 12. The properties of materials used and traffic considered in terms of cumulative axle load repetition and the thickness of each layer are tabulated in Tables 7 and 8. The following performance criteria equations were used for the design of flexible pavement as per IRC 37 2018.

$$N_R = 1.4100{*}10^{-08}[1/\varepsilon_v]^{4.5337}\text{(Subgrade rutting criteria)} \qquad (11)$$

where N_R = subgrade rutting life (cumulative Number of standard axle load repetitions); ε_v = vertical compressive strain at the top of the subgrade.

$$N_f = 0.5161{*}C{*}10^{-04}[1/\varepsilon_t]^{3.9}{*}[1/M_{Rm}] \quad \text{(Fatigue cracking Criteria for bituminous layer)} \qquad (12)$$

where C = the adjustment factor = 10^{M}, and M = 4.84

$$\left(\frac{V_{be}}{V_a + V_{be}} - 0.69\right)$$

where V_a = % volume of air voids in the bituminous mix

Table 7. Pavement design specifications and layer properties.

Factors	Provisions	Layer	Elastic Modulus, MPa	μ- value
Pavement	National Highway	BC	3000	0.35
Design traffic	131 MSA	Aggregate interlayer	450	0.35
Design period	20 years	CTB	1350 (RCA) 1500 (NCA)	0.25
Rutting model	90% Reliability	CTSB	600	0.25
Fatigue model	90% Reliability	Subgrade	62	0.35

Table 8. The results of the pavement design and analysis.

Stabilised pavement layers	Layer thickness (mm) Cement-treated recycled aggregate layers		Conventional pavement layers
Surface course	125		125
Aggregate interlayer	100		100
CTB		120 (RCA)	120
Cement treated sub-base		200 (NCA)	200
Total thickness (mm)	540		540

Table 9. Strain comparison.

Layer	Allowable microstrain IRC 37- 2018		Actual microstrain		Remarks
Bituminous layer	140	140	125	124	Safe
Cement-treated base	113 (RCA)	107 (NCA)	65 (RCA)	65 (NCA)	Safe
Subgrade	301	301	102	101	Safe

(considered value for design purpose: 3%); V_{be} = % volume of effective bitumen in the mix (considered value for design purpose: 11.5%); N_f = fatigue life of bituminous layer; ε_t = horizontal tensile strain at the bottom of bituminous layer; M_{Rm}= resilient modulus (MPa) of bituminous mix.

The two pavement sections were analysed using IITPAVE software as per IRC 37-2018 (Congress 2018). The allowable strains were calculated from Equations (11) and (12), and actual strain values in pavement layers were obtained from the analysis using IITPAVE software are tabulated in Table 9. In the case of pavements with CTB layer, fatigue performance must be assessed. The fatigue performance of the pavement was checked using the following fatigue performance model.

$$N = \mathrm{RF}\left[\frac{\left(\frac{113000}{E^{0.804}} + 191\right)}{\varepsilon_t}\right]^{12} \quad (13)$$

where RF = reliability factor for cementitious materials for failure against fatigue; RF = 1 for National Highways, Expressways and State Highways; N = Number of standard axle load repetitions which CTB can sustain; E = Elastic Modulus of CTB material (MPa); ε_t = tensile strain at the bottom of the CTB layer (microstrain). The tensile strain in the cement-treated base layer was obtained from the pavement analysis using IITPAVE software for trial thickness (Congress 2018). Hence, using Equation (13), the number of standard axles load repetitions were found to be 126 MSA which is less than the design traffic of 131 MSA, which means pavement is safe.

Conclusions

In this study, the optimisation and characterisation of the CTRCA mixes were carried out. The RSM was employed to study the effect of individual and combined factors on CTRCA mixtures. Based on test results, RCA can be used in cement-treated base and sub-base courses in Pavements. The following conclusions are drawn based on the present investigation in the laboratory.

- The mix with NCA could get the required strength in UCS, FS, ITS and Elastic Modulus at 5 per cent Cement content after seven days of curing. It also passes the durability test.
- The CTRCA mix with 30 per cent NCA and 70 per cent RCA could get the required strength with 5.8 per cent cement after seven days of curing in terms of UCS, FS, ITS and Elastic Modulus. All the samples satisfy the durability test.
- The critical observation made while conducting tests in the laboratory is that as RCA increases, the MDD decreases and OMC Increases. The NCA can be completely replaced at 7% cement. The desired strength is attained after 28 days of curing only.
- Based on the SEM and EDS analysis, it is concluded that there are many voids in the structure and the old ITZ, which is the weak spot of the matrix, indicating a significant effect on mechanical properties. The Si/Ca ratio of the CTRCA mixture was found to be 0.23, which signifies strength and durability.
- The validation of the optimum mix in the laboratory indicates that the mix can be effectively used in base and sub-base courses based on strength requirements. The optimisation results are statistically significant, evident in Table 6 and Figure 10.

Disclosure statement

No potential conflict of interest was reported by the author(s).

ORCID

A. U. Ravi Shankar http://orcid.org/0000-0002-5750-2226

References

Ä, S.B.M., *et al.*, 2012. Innovative materials and techniques in concrete construction. *Innovative Materials and Techniques in Concrete Construction*.

Aghililotf, M., Palassi, M., and Ramezanianpour, A.M., 2021. Mechanical and durability assessment of unconfined recycled concrete aggregates and natural aggregates used in road constructions. *International Journal of Pavement Engineering*, 22 (12), 1518–1530.

Agrela, F., *et al.*, 2012. Construction of road sections using mixed recycled aggregates treated with cement in Malaga, Spain. *Resources, Conservation and Recycling*, 58, 98–106.

Akhtar, A., and Sarmah, A.K., 2018. Construction and demolition waste generation and properties of recycled aggregate concrete: a global perspective. *Journal of Cleaner Production*, 186, 262–281.

Arulrajah, A., *et al.*, 2012. Geotechnical properties of recycled concrete aggregate in pavement sub-base applications. *Geotechnical Testing Journal*, 35 (5), 1–9.

Arulrajah, A., *et al.*, 2016. Stabilization of recycled demolition aggregates by geopolymers comprising calcium carbide residue, fly ash and slag precursors. *Construction and Building Materials*, 114, 864–873.

Arulrajah, A., Piratheepan, J., and Disfani, M.M., 2014. Reclaimed asphalt pavement and recycled concrete aggregate blends in pavement subbases: laboratory and field evaluation. *Journal of Materials in Civil Engineering*, 26 (2), 349–357.

ASTM C39-01, 2003. Standard test method for compressive strength of cylindrical concrete specimens 1. *ASTM Standard Book*, i (March), 1–5.

ASTM C496, 2020. Standard test method for splitting tensile strength of cylindrical concrete specimens. *Annual Book of ASTM Standards*, i, 545-545-3.

ASTM C78, 2018. Standard test method for flexural strength of concrete (using simple beam with third-point loading) 1. Hand The, C78-02 (C), 1–4. West Conshohocken, PA: ASTM International.

ASTM D1557-07, 2014. a.S.T.M D1557.Pdf. *Standard test methods for laboratory compaction characteristics of soil*.

ASTM D-559, 1996. Métodos de prueba estándar para humedecimiento y secado de mezclas compactadas de suelo y cemento, 14–19.

Aydilek.pdf, n.d.

Aydin, S., 2013. A ternary optimisation of mineral additives of alkali activated cement mortars. *Construction and Building Materials*, 43, 131–138.

Bestgen, J.O., *et al.*, 2016. Mechanical and environmental suitability of recycled concrete aggregate as a highway base material. *Journal of Materials in Civil Engineering*, 28 (9), 1–13.

Cardoso, R., *et al.*, 2016. Use of recycled aggregates from construction and demolition waste in geotechnical applications: a literature review. *Waste Management*, 49, 131–145.

Chung, S.S., and Lo, C.W.H., 2003. Evaluating sustainability in waste management: the case of construction and demolition, chemical and clinical wastes in Hong Kong. *Resources, Conservation and Recycling*, 37 (2), 119–145.

Dong, S., *et al.*, 2021. A novel method for testing the fatigue performance of cement stabilized base field coring samples. *Construction and Building Materials*, 274, 122065.

Ebrahim Abu El-Maaty Behiry, A., 2013. Utilization of cement treated recycled concrete aggregates as base or subbase layer in Egypt. *Ain Shams Engineering Journal*, 4 (4), 661–673.

Eren, Ş., and Filiz, M., 2009. Comparing the conventional soil stabilization methods to the consolid system used as an alternative admixture matter in Isparta Darıdere material. *Construction and Building Materials*, 23 (7), 2473–2480.

Gabr, A.R., and Cameron, D.A., 2012. Properties of recycled concrete aggregate for unbound pavement construction. *Journal of Materials in Civil Engineering*, 24 (6), 754–764.

George, K.P., 1990. Characterization and structural design of cement-treated base. *Transportation Research Record*, 1288, 78–87.

Haider, I., *et al.*, 2014. Evaluation of the mechanical performance of recycled concrete aggregates used in highway base layers, 3686–3694.

Hou, Y., Ji, X., and Su, X., 2019. Mechanical properties and strength criteria of cement-stabilised recycled concrete aggregate. *International Journal of Pavement Engineering*, 20 (3), 339–348.

IRC, 37, 2018. *Guidelines for the design of flexible pavements (Fourth Revision)*. IRC 37-2018. New Delhi: Indian Roads Congress.

IRC SP 89_Part 1, 2010. Guidelines for soil and granular material stabilization using cement, lime and fly ash. *Indian Roads Congress*, 53 (9), 1689–1699.

IS 4332 Part 4, 1968. Methods of test for stabilized soils Part IV wetting and drying, and freezing and thawing tests for compacted soil-cement mixtures. *IS 4332 (Part 4)*, New Delhi.

IS 5816, 1999. Indian standard splitting tensile strength of concrete-method of test. *Bureau of Indian Standards*, 1–14.

Jayakody, S., Gallage, C., and Ramanujam, J., 2019. Performance characteristics of recycled concrete aggregate as an unbound pavement material. *Heliyon*, 5 (9), e02494.

Jofre, C., and Kraemer, C., 2008. *Manual of soil stabilization with cement or lime*. Madrid: Spanish Institute of Cement and its Applications (SICA).

Kockal, N.U., and Ozturan, T., 2011. Optimization of properties of fly ash aggregates for high-strength lightweight concrete production. *Materials & Design*, 32 (6), 3586–3593.

Leite, F.D.C., *et al.*, 2011. Laboratory evaluation of recycled construction and demolition waste for pavements. *Construction and Building Materials*, 25 (6), 2972–2979.

Li, Z., Lu, D., and Gao, X., 2021. Optimization of mixture proportions by statistical experimental design using response surface method – a review. *Journal of Building Engineering*, 36 (September 2020), 102101.

Lim, S., and Zollinger, D.G., 2003. Estimation of the compressive strength and modulus of elasticity of cement-treated aggregate base materials. *Transportation Research Record: Journal of the Transportation Research Board*, 1837, 30–38.

Maduabuchukwu Nwakaire, C., *et al.*, 2020. Utilisation of recycled concrete aggregates for sustainable highway pavement applications; a review. *Construction and Building Materials*, 235, 117444.

Martinez-Conesa, E.J., *et al.*, 2017. Optimization of geometric parameters in a welded joint through response surface methodology. *Construction and Building Materials*, 154, 105–114.

Mermerdaş, K., *et al.*, 2017. Optimization of lightweight GGBFS and FA geopolymer mortars by response surface method. *Construction and Building Materials*, 139, 159–171.

Mohammadinia, A., *et al.*, 2015. Laboratory evaluation of the use of cement-treated construction and demolition materials in pavement base and subbase applications. *Journal of Materials in Civil Engineering*, 27 (6), 1–12.

Mohammadinia, A., *et al.*, 2016. Stabilization of demolition materials for pavement base/subbase applications using fly ash and slag geopolymers: laboratory investigation. *Journal of Materials in Civil Engineering*, 28 (7), 04016033.

Mohammadinia, A., *et al.*, 2019a. Small-strain behavior of cement-stabilized recycled concrete aggregate in pavement base layers. *Journal of Materials in Civil Engineering*, 31 (5), 04019044.

Mohammadinia, A., *et al.*, 2019b. Flexural fatigue strength of demolition aggregates stabilized with alkali-activated calcium carbide residue. *Construction and Building Materials*, 199, 115–123.

Mohammed, B.S., *et al.*, 2017. Evaluation of nano-silica modified ECC based on ultrasonic pulse velocity and rebound hammer. *The Open Civil Engineering Journal*, 11 (1), 638–649.

Mohammed, B.S., *et al.*, 2019. Optimization and characterization of cast in-situ alkali-activated pastes by response surface methodology. *Construction and Building Materials*, 225, 776–787.

MoRTH, 2013. Specifications for road bridge works 5th revision. *Indian Roads Congress on Behalf of the Govet. of India, Ministry of Road Transport & Highway*, 1, 1–883.

Nataatmadja, A., and Tan, Y.L., 2001. Resilient response of recycled concrete road aggregates. *Journal of Transportation Engineering*, 127 (5), 450–453.

Peng, Z., and Qingfu, L., 2009. Effect of polypropylene fibre on mechanical and shrinkage properties of cement-stabilised macadam. *International Journal of Pavement Engineering*, 10 (6), 435–445.

Poon, C.S., and Chan, D., 2006. Feasible use of recycled concrete aggregates and crushed clay brick as unbound road sub-base. *Construction and Building Materials*, 20 (8), 578–585.

Rahman, M.A., *et al.*, 2014. Resilient modulus and permanent deformation responses of geogrid-reinforced construction and demolition materials. *Journal of Materials in Civil Engineering*, 26 (3), 512–519.

Rezaifar, O., Hasanzadeh, M., and Gholhaki, M., 2016. Concrete made with hybrid blends of crumb rubber and metakaolin: optimization using response surface method. *Construction and Building Materials*, 123, 59–68.

Shi, X., *et al.*, 2022. Response surface methodology for multi-objective optimization of fly ash-GGBS based geopolymer mortar. *Construction and Building Materials*, 315 (October 2021), 125644.

Tang, W.C., *et al.*, 2018. Influence of red mud on fresh and hardened properties of self-compacting concrete. *Construction and Building Materials*, 178, 288–300.

Toka, E.B., and Olgun, M., 2021. Performance of granular road base and sub-base layers containing recycled concrete aggregate in different ratios. *International Journal of Pavement Engineering*, 23 (11), 3729–3742.

Usman Kankia, M., *et al.*, 2021. Effects of petroleum sludge ash in fly ash-based geopolymer mortar. *Construction and Building Materials*, 272, 121939.

Yaowarat, T., *et al.*, 2022. Cement stabilisation of recycled concrete aggregate modified with polyvinyl alcohol. *International Journal of Pavement Engineering*, 23 (2), 349–357.

Yeo, R., 2008. *The development and evaluation of protocols for the laboratory characterisation of cemented materials*.